MICROSTRUCTURAL CHARACTERIZATION OF THE HAZ OF THE AISI-439 WITH DIFFERENT HEAT INPUT

Lorena de Azevedo Silva, lorenadeazevedo@yahoo.com.br
Luciana Iglésias Lourenço Lima, lil@cdtn.br
Mônica Maria de Abreu Mendonça Schvartzman, monicas@cdtn.br
Wagner Reis da Costa Campos, wrcc@cdtn.br
Centro de Desenvolvimento da Tecnologia Nuclear (CDTN) / Comissão Nacional de Energia Nuclear (CNEN), Serviço de Integridade Estrutural (EC2) / Laboratório de Metalografia, Rua Professor Mário Werneck s/nº, Campus Universitário da UFMG, Pampulha, 30123-970 Belo Horizonte, Minas Gerais, Brasil.

Alexandre Queiroz Bracarense, bracarense@ufmg.br
Universidade Federal de Minas Gerais (UFMG) / Departamento de Engenharia Mecânica (DEMEC), Av. Antônio Carlos 6627, Campus Universitário da UFMG, Pampulha, 31270-901, Belo Horizonte, Minas Gerais, Brasil.

Abstract. *Ferritic stainless steels have certain useful corrosion properties, such as resistance to chloride, corrosion in oxidizing aqueous media, oxidation at high temperatures, etc. It is suitable for the aqueous chloride environments, heat transfer applications, condenser tubing for fresh water power plants, food-handling uses and industrial buildings, and sometimes in these applications the use of welding processes is necessary. In this paper, the relationship between the of microstructure and Vickers microhardness profile in the Heat Affect Zone (HAZ) of the ferritic stainless steels type AISI-439, for two different weld heat input, using the austenitic stainless steels type AISI-308L-Si as filler metal, was evaluated. The grain size in base metal was determined by Quantikov analyzer and in the HAZ was determined by the linear intercept method, Heyn's method. The microhardness profile was determined using Vickers microhardness measurement with 100 grams (HV-0.1). The base metal showed a ferritic matrix, a little perlite and a random distribution of the carbides and nitrite precipitate. The HAZ size, grain size, and the amount of carbides and nitrites increased to the highest heat input welding. The coarse grain favor a reduction in the hardness, however an increasing of the hardness occur in the sample with a higher heat input, due to the increase in the precipitation. It was observed that the grain size is related with heat input, and that the hardness is stronger related with other feature, as precipitation.*

Keywords*: AISI 439, ferritic stainless steel, microhardness, grain size,* heat affect zone, *HAZ.*

1. INTRODUCTION

In essence, stainless steel is low carbon content steel to which chromium is added. The minimum chromium content of the standardized stainless steels is 10.5 %. Chromium makes the steel "stainless" this means improved corrosion resistance. It is the addition of this element that affords the product a high resistance to corrosion. The chromium in the stainless steel combines in the atmosphere with oxygen to form a thin and invisible layer of chromium-containing oxide, called the passive film, this oxide is very effective to reduce the corrosion. If damaged (mechanically or chemically) this passive film regenerates, hence restoring the resistance-to-corrosion feature (Acesita, 2004, Mantel et al., 1990).

Stainless steel is a remarkable versatile material with many applications such as heat transfer applications, condenser tubing for fresh water power plants, food-handling uses and industrial buildings, chemistry, nuclear and petroleum industries. The absolutely most important property of stainless steel is the ability to maintain the same surface, colour and structure, i.e., its corrosion resistance. In many situations galvanic protection or painting of a mild steel surface is impractical (Acesita, 2004).

Many types of stainless steels have been developed to resist different corrosion environments and working conditions ensuring that factories are safe, structures last longer and our food is hygienic.

Among various applications, stainless steels are today widely used in exhaust line systems to improve the service life of automotive exhaust components, specially the upstream part of the exhaust line, manifolds and mufflers; residential furnace primary heat exchangers; direct-fired hot water tanks; heat exchanger tubing, down-pipe, converter shell, where temperatures can reach 1100 °C. Austenitic stainless steels like AISI 300 series are traditionally used, but in the last decades, the ferritic stainless steels have been developed for those applications (Vicentini, 2004, Inoue, 2003, Mantel et al., 1990 and Fujita et al., 1989).

The ferritic stainless steels are, in principle, ferritic at all temperatures. Another characteristic that distinguishes ferritic steel from austenitic material is that ferritic steels have much lower strain hardening. Ferritic stainless steels have chromium levels that range from 10.5 % to 40 % (typically 12 % or more) and carbon levels less than 0.20 %. The most common of the ferritic stainless steels are 12 % and 17 % chromium containing. Ferritic stainless steels containing no nickel as an alloying element have advantages that their production cost is low and they are free from various types of stress corrosion cracking (Campbell, 1992, Sabioni et al., 2003).

The ferritic stainless steels have several disadvantages, when welding their corrosion resistance and mechanical properties are poor, thus they have been restricted in their application, particularly in application such as chemical plants where high degree of material reliability are required (Sabioni et al., 2003).

Ferritic stainless steels with 12 % chromium are used mostly in structural applications, and with more than 17 % chromium are used in housewares, boilers, washing machines and indoor architecture, and in many of these applications the use of welding processes is necessary.

1.1. Ferritic stainless steels AISI 439

The composition of the ferritic stainless steel type AISI 439 has been balanced to provide a completely ferritic structure at all temperatures, to avoid the loss of ductility after welding and to provide resistance to intergranular corrosion. The ferritic stainless steels AISI 439 with 18-20 % chromium contains titanium and niobium for carbon and nitrogen stabilization, to prevent the risks of intergranular corrosion of weldments, due to the formation of stable titanium and niobium nitrides and carbides instead of nonstable chromium carbides. This steel is resists chloride stress corrosion cracking. This grade is suitable for equipment exposed to the aqueous chloride environments, heat transfer applications, condenser tubing for fresh water power plants, food-handling uses and water tubing for domestic and industrial buildings (Allegheny Ludlum, 2006).

The ferritic stainless steel type AISI 439 is used in a wide variety of applications in the power generation, petroleum refining and chemical process industries as heat exchanger tubing, in the residential furnace market, in some small hot water tank applications and automotive exhaust manifolds and mufflers (Allegheny Ludlum, 2006).

The stainless steel type AISI 439 can be welded under strict precautions using all standard arc welding process. They can be jointed with welding consumables that match or near match the base metal or with austenitic welding consumable, for example electrode AISI 308L-Si and AISI 316L-Si wires. During welding, ferritic stainless steel grades can suffer a loss of ductility due to grain growth, martensite formation and carbide precipitation (Allegheny Ludlum, 2006).

1.2. Weldability of ferritic stainless steels

When the ferritic stainless steel are welding, the chromium carbide and nitrite precipitation can occur and lead to intergranular attack if it occurs in the sensitization temperature range of about 500-800 °C. This precipitation will occur in the very low interstitial range as well as at higher levels. In this stainless steel, titanium nitrite has very low solubility in ferrite and exists as a stable phase at all temperatures below the solidus. However, substantial solubility exists for the titanium carbide and the niobium nitrite and carbide above about 1100 °C. At lower temperatures, titanium, niobium and chromium carbide and nitrite precipitation can occur but will not generally produce sensitization if it occurs above about 800 °C. Thus, annealing treatments and successful welding are based on this sensitization effect (Allegheny Ludlum, 2006).

In some ferritic stainless steel, when cooling down from temperatures above 900 °C, the sensitization to intergranular corrosion is likely to occur and welded joints are often less ductile and has a higher hardness than the base material, due to ferrite grain growth and martensite formation. Special attention should be required in order to avoid the embrittlement in weldments. Using low heat input, and occasionally warming the part before welding can reduce this embrittlement. It is known, however, that excessively high weld heat input may not be beneficial due to the risk of intermetallic phase precipitation and grain growth, both of which reduce impact toughness (Russel, 2005).

The welding is carried through with the located application of heat, and therefore, can occur alterations in the properties of the material, nor always desirable. Many of these alterations occur during the solidification and cooling of the weld, and they are related to the initial microstructure of the material.

In the heat affected zone significant changes in microstructure and properties can be occurring due to the induced transformations for the thermal cycle of welding. The grain growth region corresponds to the region of the HAZ that was warm until the field of coexistence of the austenite and the ferrite. An intense grain growth and the dissolution and posterior precipitation of the carbides and nitrites characterize it. In general way, the welding is characterized by a structure of the grain coarse; presenting a net of martensita near the boundary grain and carbide and nitrite precipitated inside the grains, these increase the hardness (Lancaster, 1999, Modenesi, 2001).

The grain growth and the width of the heat affect zone can be reduced by the use of low energy of welding and by choice of an adequate process or procedure of welding. The low speed cooling of the welding promotes a great grain of the HAZ and the precipitation embrittlement. On the other hand, a welding with the high speeds cooling promotes an increase in the amount of ferrite in the heat affect zone and thus, a loss of toughness. Thus, the cooling condition for weld of this steel must be looked (Lancaster, 1999, Modenesi, 2001).

In this paper, the relationship between the grain size profile measurement by the modifier Heyn's method and the microhardness profile using Vickers microhardness measurements, of the heat affect zone of the ferritic stainless steel AISI 439 welded by GMAW, with different weld heat input using the AISI 308L-Si wire as filler metal, were evaluated.

3. EXPERIMENTAL DETAILS

3.1. Material

The base metal using the ferritic stainless steel AISI 439 plates of dimensions of 300 x 100 x 1.5 mm, as-received condition. The manual Gas Metal Arc Welding (GMAW) process using argon shielding gas, was performance. The filler metal wire, an austenitic stainless steel type AISI 308L-Si with 1.2 mm diameter was used for welding. The chemical compositions of the base metal and the filler metal are presented in Tab. 1 and 2.

Table 1. Chemical Composition of the AISI 439 Stainless Steels (Acesita, 2004).

Chemical Composition (% W)									
C	Mn	P	S	Si	Ni	Cr	Mo	Al	Ti
0,0095	0,1434	0,0234	0,0027	0,4032	0,1777	17,1283	0,0191	0,0115	0,1984

Table 2. Chemical Composition of the filler metal AISI 308 L-Si.

Chemical Composition (% W)				
C	Mn	Si	Ni	Cr
0.08	1.70	0.5	10	21

3.2. Welding

In welding, by GMAW process, the argon gas flow was kept constant at 20 L/min, using a direct current power source. Bead-on-plate weld on AISI 439 steel plates using ER 308L-Si as welding filler metal and the following argon shielding gas was performed. Two different heat inputs welding (299 and 632 J/mm) were used. The welding parameters were chosen in order to obtain the better transfer mode; the optimized parameters are shown in Tab. 3.

Table 3. The gas metal arc welding optimized parameters.

Sample	Current (A)	Welding Velocity (mm/s)	Voltage (V)	Heat Input (J/mm)	Flow gas (L/min)
1	110	7	19	299	20
2	133	4	19	632	20

3.3. The specimens preparation

The metallographic examination of each sample was carried out to characterize the base metal and the HAZ. Microhardness testing and metallographic analyses were performed. The specimens were prepared across the top surface of the weldment. To guarantee the flatness minimizing edge rounding of the polished surface, hot mounting was accomplished using a Bakelite resin. The mounted specimens were wet ground through a series of silicon carbide papers up to 2000 mesh grit. Final polishing was accomplished on a cloth-covered with diamond solution up to 1μm.

The specimens for metallographic analyses were submitted to chemical etching with Vilella's reagent (100 ml ethanol, 1 g picric acid, 10 ml hydrochloridric acid) for 90 seconds in order to reveal microstructural details. The samples were then examined in a Leitz optical microscope, outfitted with a Sony Digital Camera, used in performing the optical metallography and a JEOL microprobe analysis to energy depressive spectroscopy (EDS).

3.4. Grain size measurement

The Quantikov software analyzer was used to determine the grain size in base metal. This software is based on Saltykov method (Pinto, 1996). The measurement of grain size profile in HAZ was made by linear intercept method according to an adaptation of the Heyn's method. In this method, one or more lines are superimposed over the structure at a known magnification. The true length of line is divided by the number of grains intercepted by the line. This gives the average length of the intercepted grains within the line, the average grain size, for the each line (Lima, 2007).

3.5. Microhardness measurement

The microhardness profiles were performed in order to characterize the extent of the HAZ. The microhardness, in Vickers' hardness scale, was measured across the polished top surface of the weldment for a load of 100 g (HV-0.1).

4. RESULTS AND DISCUSSION

4.1. Micrography

The typical base metal microstructure of the ferritic stainless steel type AISI 439, as-received condition, studied here is shown in Fig. 1. The microstructure consisting of grains of ferrite and a little perlite in the ferrite boundary grain with some precipitated into the ferrite grain.

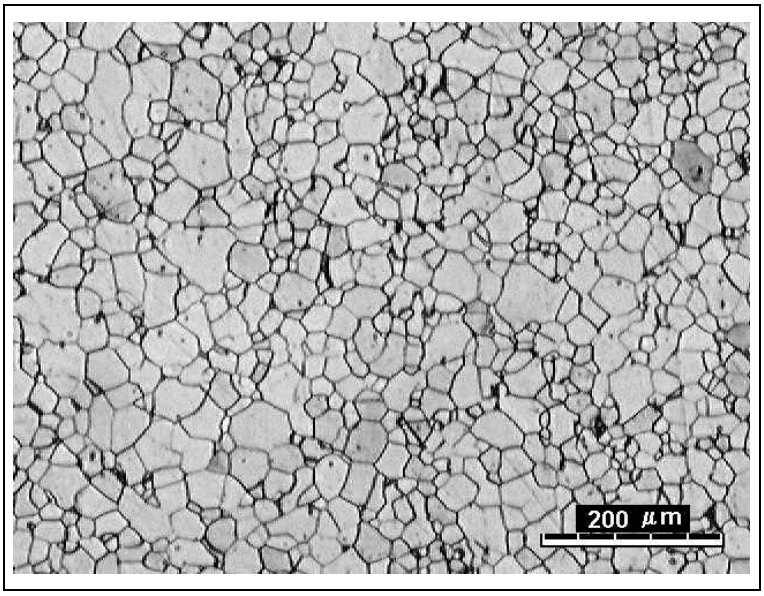

Figure 1 - Micrography of the base metal AISI 439, as-received condition, ferritic grain with some carbide (fine dark point) into the grain and perlite (black spot) in grain boundary. Attack Villela's reagent.

The HAZ of the AISI 439 showed a microstructure consisting of equiaxial ferrite grains with coarse-grained structure with large variations in size and many precipitate, Fig. 2 (a) low and (b) high weld heat input (299 and 632 J/mm). In both HAZ microstructures were found an increase in the amount of precipitate, but to the higher weld heat input the amount of precipitate was more increase.

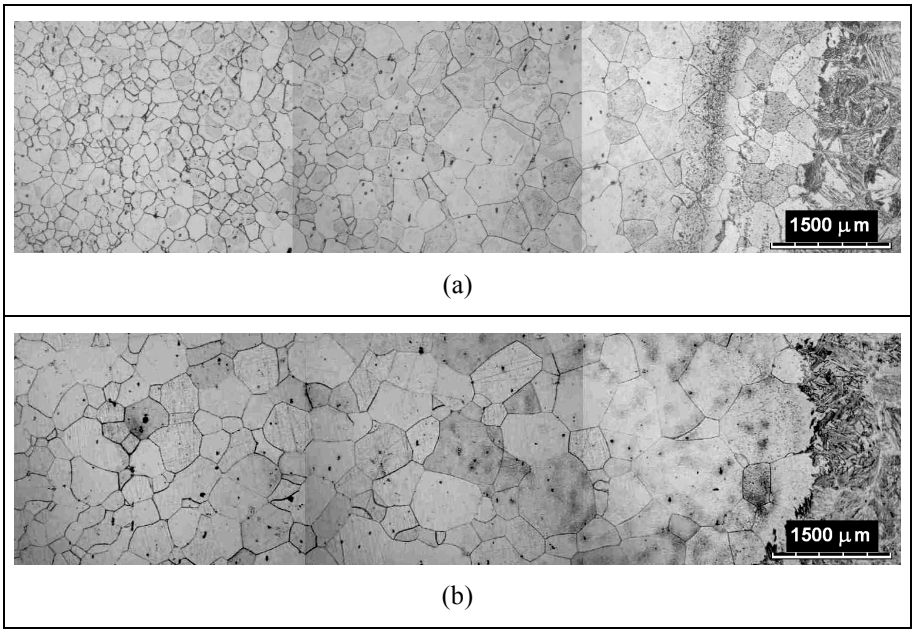

Figure 2. Micrography of the HAZ, (a) low heat input (299 J/mm) and (b) high weld heat input (632 J/mm). Attack Villela's reagent.

4.2. Determination of the grain size in HAZ

4.2.1. Grain size in base metals

Samples of the base metal were prepared for examination with a metallurgical microscope. The average grain size of the base metal by the Saltykov method using the Quantikov software analyzer was determined. The average grain size measurement in the base metal was 23.8 μm.

4.2.2. Grain size in HAZ

Grain size in HAZ was determined using a modifier intercept method (Heyn's method) described below. Parallel straight lines, all of the same length, were superimposed on the HAZ photomicrography, see Fig. 3. The number of grains boundary intersected by each line segment was counted. The true line length was then divided by number of grains boundary intersected by each parallel straight line. For each line was determined the grain size, and each parallel straight line represent a distance from the fusion line, so that the profile grain size versus distance of the parallel straight line from fusion line (Lima, 2007).

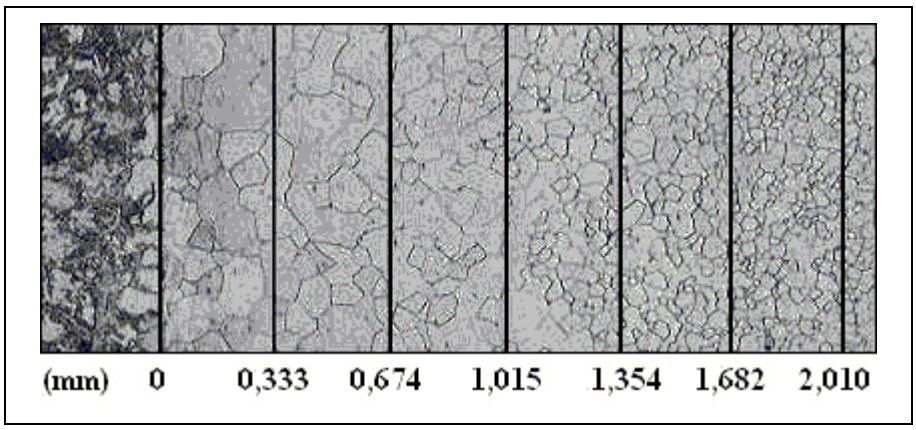

Figure 3. Parallel straight lines of the same length were superimposed on the HAZ photomicrography from the fusion line in the HAZ to the base metal.

The HAZ grain size was determined for Eq. 1.

$$Y = \frac{L}{N} \tag{1}$$

Where:

Y: grain size determined by Heyn's method;
L: true line length of measurement;
N: number of grains boundary intersected by line.

4.2.3. Determination of the grain size profile in HAZ

The variation of grain size, determined using the modifier Heyn's method, in relationship with the distance from the fusing line in HAZ was best described by first-order exponential decline curves and can be represented by equation:

$$Y = Y_0 + A.e^{R_0.X} \tag{2}$$

Where:

Y : Grain size (μm);
Y_0 : Grain size of the base metal (23.8 μm);
X : Distance until the fusing line in HAZ (mm);
A and R_0 : Adjust parameters.

Figures 4 and 5 shown the grain size variation in relationship with the distance from the fusing line in heat affect zone (ZTA), for the two different weld heat input (299 and 632 J/mm), in according with Eq. (2).

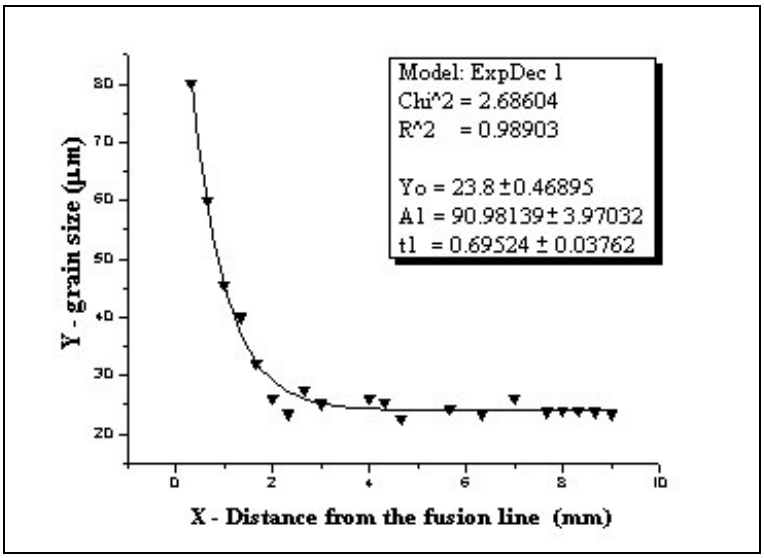

Figure 4. Grain size profile in relationship with the distance from the fusing line in HAZ, low heat input 299 J/mm.

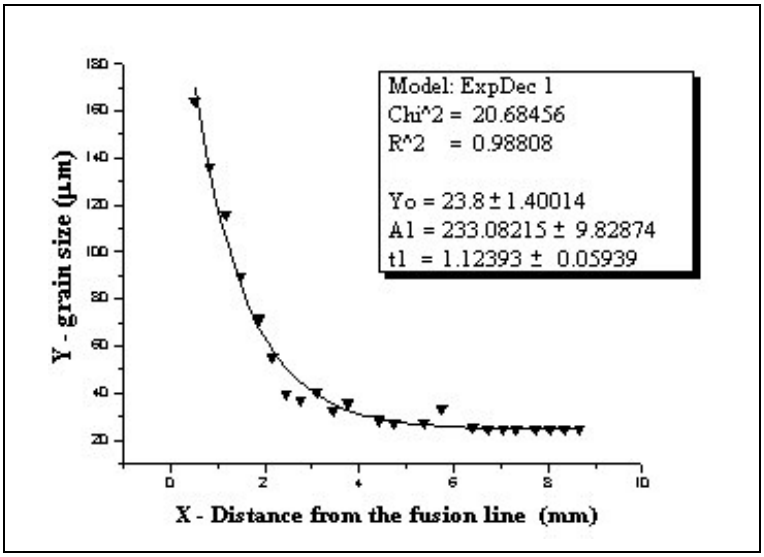

Figure 5. Grain size profile in relationship with the distance from the fusing line in HAZ, high heat input 632 J/mm.

All samples welded with low heat input 299 J/mm or heat input 632 J/mm showed an increase the grain size in heat affect zone (HAZ). It can be observed that in both the curves, Fig. 4 and 5, the grain size decline until to acquire a natural variation of each steel sample about 23,8 µm. They were get the 4.2 mm for low heat input and 5.6 mm for high heat input.

Grain size profile measurements of HAZ showed increasing grain size with increasing heat input. The sample with high heat input presented higher grain size values then to low heat input near to the fusion line. The decline of the grain size was more accented for the low heat input. The grain size of the HAZ is observed to increase as well, due to time in high temperature the samples remain.

4.2.4. Determination of the Vickers microhardness profile in HAZ

Vickers microhardness profiles at a load of 100 g (HV-0.1) were performed. The variation of Vickers microhardness with the distance from the fusing line in HAZ was best described by second-order exponential decline curves, and can be represented by Eq. (3):

$$Y = Y_0 + A_1.e^{-X/t1} + A_1.e^{-X/t2} \tag{3}$$

Where: Y : Vickers microhardness;
Y_0 : Vickers microhardness of the base metal (149 HV-0.1);
X : Distance until the fusing line in HAZ (mm);
A_1, A_2, t_1, t_2, and R_0: Adjust parameters.

Figures 6 and 7 shown the Vickers microhardness variation in relationship with the distance from the fusing line in HAZ, for two different weld heat input (299 and 632 J/mm), in according with Eq. (3).

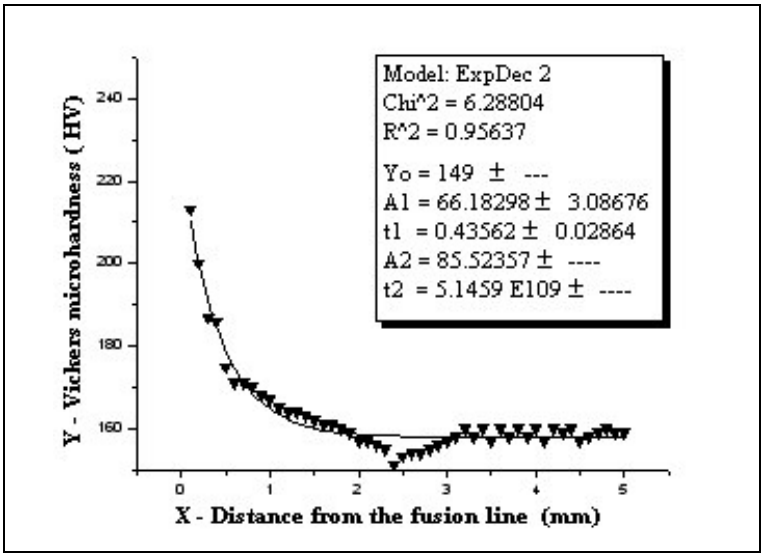

Figure 6. Curves Vickers microhardness variation in relationship with the distance from the fusing line in HAZ, low heat input 299 J/mm.

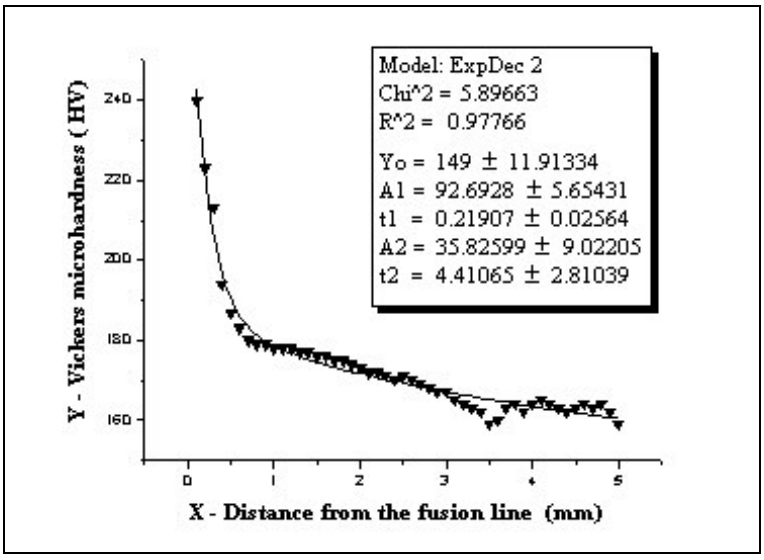

Figure 7. Curves Vickers microhardness variation in relationship with the distance from the fusing line in HAZ, high heat input 632 J/mm.

All samples welded with 299 J/mm or 632 J/mm heat input showed an increase the hardened. It can be observed that in both the curves the microhardness decline until reaching a minimum value, increasing after until to acquire a natural variation of each steel sample about 149 HV-0.1. The distance from the fusing line where each sample reaches its minimum value of microhardness was of the 2.4 mm for low heat input and 3.5 mm for high heat input.

Vickers microhardness profile, with 100 grams load, measurements of ferritic stainless steel HAZ showed increasing hardness with increasing weld heat input. The sample with higher weld heat input presented higher Vickers microhardness values then the low weld heat input near to the fusion line.

The decline of the Vickers microhardness was more accented for the sample with the low weld heat input. The microhardness of the HAZ is observed to increase as well, due to precipitation of the alloying elements present in the steel.

Although the growth of the ferritic grains to favor a reduction in the microhardness, in welding process, the carbides precipitation increase the hardness in HAZ, that occurred in highest amount with a highest heat input, as illustrated in Fig. 6 and 7.

4.5. Precipitate analysis

The chemical composition of the precipitates was qualitatively analyzed using energy-dispersive spectroscopy (EDS) in a microprobe. Figure 8 shown the EDS spectrum analysis in HAZ precipitates, (a) some titanium carbide and nitrite precipitate with Al and Mg oxide inclusion, and (b) chromium carbide precipitate.

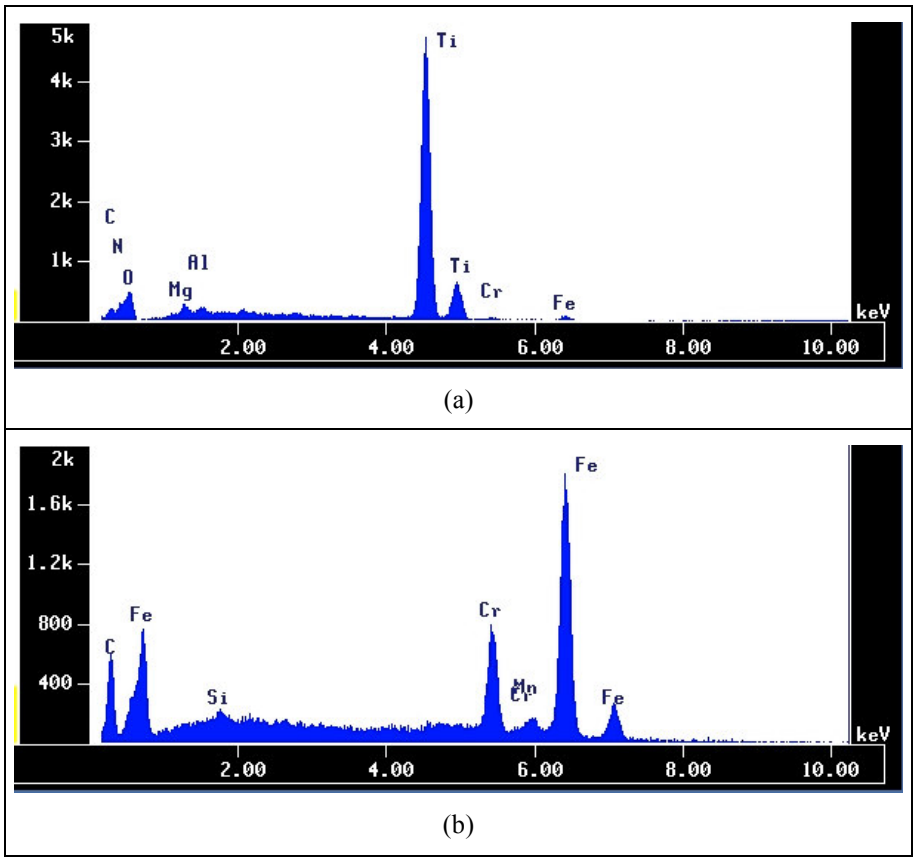

Figure 8. EDS spectrum in HAZ precipitated, (a) some titanium carbide and nitrite precipitate with Al and Mg oxide inclusion in matrix and (b) chromium carbide precipitate in grain boundary.

5. CONCLUSIONS

The base metal AISI 439 showed a ferritic matrix, with a little perlite, and a random distribution of the carbides and nitrite precipitates. After welding, the HAZ size, the HAZ grain size, and the amount of carbide and nitrite precipitates had a significantly increase, more intense to the highest weld heat input.

Although the coarse grain to be suitable to promote a reduction in the hardness, the precipitation occurred in highest amount the sample with the higher weld heat input, had increase the microhardness. It was observed that the grain size is related with heat input, and that the microhardness this more strong related with other feature, as precipitation.

The HAZ size obtained by the modifier Heyn's method showed that the distance from the fusion line where each sample reaches a minimum grain size value close to those in the base metal, 23.8 μm, was 4.2 mm for low heat input, and 5.6 mm for high heat input.

The HAZ size obtained by Vickers microhardness measurement, showed that the distance from the fusion line up to point where each sample reaches a minimum microhardness value close to those in the base metal, 149 HV-0.1, was 2.4 mm for low heat input and 3.5 mm for high heat input.

The HAZ size measurement showed the best on the grain size measurement then the microhardness.

7. ACKNOWLEDGEMENTS

The study presented in this paper was part of the Master of Science by Luciana I. L. Lima performed at Federal University of Minas Gerais - Mechanical Engineering Department. The authors gratefully acknowledge the technical and financial support of CDTN/CNEN in this study. The authors also thank Fundacao de Amparo a Pesquisa do Estado de Minas Gerais – FAPEMIG, that partially supported the development and the presentation of this work.

8. REFERENCES

Acesita - Cia de Aços Especiais Itabira, 2004. "Manual Técnico de Aços Inoxidáveis – Características Básicas e cuidados".

Allegheny Ludlum, 1999, "Blue Sheet - Technical Data Stainless Steels Type 439/AL 439HP" - Sep. 2006, <http://www.nksteel.com/KOREA/front/439/AL439.pdf>.

Campbell, R. D., 1992, "Ferritic Stainless Steel Welding Metallurgy", Key Engineering Materials, Vol. 69 & 70, pp. 167-216.

Fujita, N.; Ohmura, K.; Kikuchi, M.; Suzuki, T.; Funaki, S.; Hirishige, I., 1989, Scripta Met., No. 32 (5/6), pp. 449-469.

Inoue, Y. and Kikuchi, M., July 2003, Present and Future Trends of Stainless Steel for Automotive Exhaust System. Nippon Steel Technical Report No.88, pp. 62-70.

Lancaster, J.F., 1999, "Metallurgy of Welding", Abington Publishing, 6th Ed., Cambridge, England, pp. 446.

Lima, L. I. L., 2007, "Metodologia para Avaliação da Corrosão da Zona Termicamente Afetada de Aço Inoxidável Ferrítico AISI 439 Soldado", Dissertação de mestrado, Escola de Engenharia Mecânica - UFMG.

Mantel, M.; Baroux, B.; Ragot, J.; Chemelle, P., 1990, "Mémoire et Etudes Scientifiques", Revue de Métallurgie, pp. 637-648.

Modenesi, P.J., 2001, "Soldabilidade dos Aços Inoxidáveis - Metalurgia da Soldagem dos aços Inoxidáveis Ferríticos", Senai-SP, Coleção Tecnologia da Soldagem, Vol. 1, pp. 27-30.

Pinto, L. C. M., 1996, "Quantikov – Um analisador Microestrutural para um ambiente Windows™", Tese de Doutorado. Universidade de São Paulo/ Instituto de Pesquisas Energéticas e Nucleares – USP/IPEN.

Russell, S. W. and Lundin, C. D., 2005, "The Development of Qualification Standards for Cast Duplex Stainless Steel". Materials Joining Group, Materials Science and Engineering, The University of Tennessee, Knoxville. Final Report Vol. 2. Submitted to U. S. Department of Energy, Award Number - DE-FC36-00 ID13975 Oct. 1, 2000 – Sep. 30, 2005.

Sabioni, A. C. S., Huntz, A. M., Luz, E. C., Mantel, M., Haut, C., 2003, "Comparative Study of High Temperature Oxidation Behaviour in AISI 304 and AISI 439 Stainless Steels", Materials research, Vol. 6, No. 2, pp. 179-185.

Vicentini, B, Sinigaglia, D., Taccani, G., Rondelli, G., Gherardi, F. and Ortali, P. L., Oct. 2004, "New stainless steels for sea water applications. Part. 1: Corrosion and mechanical properties of ferritic stainless steels". Materials and Corrosion, Vol. 33, Issue 3, pp. 132-143.

9. RESPONSIBILITY NOTICE

The authors are the only responsible for the printed material included in this paper.